Glucose Directly Links to Lipid Metabolism through High Affinity Interaction with Peroxisome Proliferator-activated Receptor α*

Heather A. Hostetler[‡]**, Huan Huang**[‡]**, Ann B. Kier**[§]**, and Friedhelm Schroeder**[‡1]

From the Departments of [‡]*Physiology and Pharmacology and* [§]*Pathobiology, Texas A&M University, College Station, Texas 77843-4467*

The pathophysiology of diabetes is characterized not only by elevated glucose but also elevated long chain fatty acid levels. We show for the first time that the peroxisome proliferator-activated receptor-α (PPARα) binds glucose and glucose metabolites with high affinity, resulting in significantly altered PPARα secondary structure. Glucose decreased PPARα interaction with fatty acid metabolites and steroid receptor coactivator-1 while increasing PPARα interaction with DNA. Concomitantly, glucose increased PPARα interaction with steroid receptor coactivator-1, DNA binding, and transactivation of β-oxidation pathways in the presence of activating ligands. Heterodimerization of PPARα to the retinoid X receptor-α resulted in even larger increases in transactivation with the addition of glucose. These data suggest that PPARα is responsible for maintaining energy homeostasis through a concentration-dependent regulation of both lipids and sugars and that hyperglycemic injury mediated by PPARα occurs not only indirectly through elevated long chain fatty acid levels but also through direct action of glucose on PPARα.

Energy homeostasis is a highly complex and strictly regulated process. Free fatty acids compete with glucose for oxidation, and increased free fatty acid concentrations are associated with reduced muscle glycogen synthesis. Dysregulation at any step may elicit severe pathophysiological complications, as seen in diabetes. Maintained low levels of blood glucose are critical for preventing or delaying the clinical complications of diabetes, such as insulin resistance and cardiovascular disease (1). Although the liver plays essential roles in the control of blood glucose levels by modulating gluconeogenesis and glycogen synthesis, the specific mechanism(s) of this regulation is unclear. Several studies suggest that peroxisome proliferator-activated receptor α (PPARα),[2] a ligand-regulated transcrip-

tion factor belonging to the nuclear hormone receptor superfamily, contributes to this regulation.

PPARα is highly expressed in liver and is the target of potent hypolipidemic drugs, such as fibrates, used to treat cardiovascular disease (2). Although a variety of compounds bind and activate PPARα, long chain fatty acids (LCFA) and their metabolites (*i.e.* long chain fatty acyl-CoAs, LCFA-CoA) function as high affinity, endogenous ligands (3–5), which could play an important role because diabetes is characterized not only by elevated glucose levels but also elevated LCFA and LCFA-CoA levels (6). Ligand binding initiates PPARα transcription of multiple genes in fatty acid and glucose metabolism while concomitantly down-regulating genes in insulin signaling (7–9). Furthermore, expression of PPARα is elevated in humans with type 2 diabetes (10), and PPARα-null mice are protected from high fat diet-induced insulin resistance (11).

EXPERIMENTAL PROCEDURES

Protein Expression and Purification—The bacterial expression vector containing murine PPARα (pET-PPARαΔAB) was expressed in the BL21(DE3)pLysS strain of *Escherichia coli* as described (3) and purified by cation exchange and size exclusion chromatography. Dialyzation, quantification, and protein quality were analyzed as previously described (4). This truncated version, rather than the full-length protein, was used for the pure protein studies because of solubility issues with the full-length protein and difficulties with its recombinant purification. Although this recombinant protein was lacking the A/B domain, the entire DNA-binding domain and ligand-binding domain were present. This truncated version is expected to show ligand binding properties identical to those of the full-length receptor based upon similar experiments with PPARγ (12, 13). However, the A/B region of PPARα has been found to have a transactivating function through the ligand-independent transactivation domain (AF-1 activity) (14), and for this reason, the full-length protein was used for the coimmunoprecipitation, DNA binding, and transactivation assays.

Glucose Binding Assay—The direct binding of glucose and the glucose metabolites (glucose-1-phosphate, G-1-P; glucose-6-phosphate, G-6-P) to 100 nM PPARαΔAB was determined by quenching of intrinsic PPARαΔAB aromatic amino acid fluo-

[1] To whom correspondence should be addressed: Dept. of Physiology and Pharmacology, Texas A & M University, TVMC, College Station, TX 77843-4466. Tel.: 979-862-1433; Fax: 979-862-4929; E-mail: fschroeder@cvm.tamu.edu.

[2] The abbreviations used are: PPARα, peroxisome proliferator-activated receptor α; LCFA, long chain fatty acid; SRC-1, steroid receptor coactiva-

tor-1; RXRα, retinoid X receptor α; G-1-P, glucose-1-phosphate; G-6-P, glucose-6-phosphate; PPRE, peroxisome proliferator response element; L-FABP, liver fatty acid-binding protein; DMEM, Dulbecco's modified Eagle's medium; PBS, phosphate-buffered saline; LSCM, laser scanning confocal microscopy.

rescence as previously described for nonfluorescent fatty acids and fatty acyl-CoAs (4, 5). Emission spectra from 300 to 400 nm were obtained at 24 °C by excitation at 280 nm with a PC1 photon counting spectrofluorometer (ISS Inc., Champaign, IL). The data were corrected for background (buffer, fluorescent ligands, and solvent effects), and the maximal intensities were used to calculate the dissociation constant (K_d) and the number of binding sites as previously described (4).

Autoglycation—To determine whether PPARα autoglycation could occur under the conditions of the binding and circular dichroism assays, 100 nM PPARαΔAB was incubated with 1 μM 2-deoxy-d-[1-^{3}H]glucose supplemented with cold glucose for a final concentration of 20 mM at room temperature for 30 min in PBS. Following incubation, the mixture was applied to a filtration device (Microcon; Millipore, Bedford, MA) and centrifuged to remove free glucose. The resulting protein-glucose mixture was washed three times with excess glucose to determine whether the radioactive glucose was permanently bound (covalent) or could be removed. Each flow-through and retentate was examined for activity with a scintillation counter as compared with no protein controls.

Circular Dichroism—Circular dichroic spectra of 0.8 μM PPARαΔAB were taken in the absence and presence of glucose and glucose metabolites with a J-710 spectropolarimeter (JASCO Inc., Easton, MD) as previously described (4, 5). Glucose concentrations below (0.6 μM) and above (6 μM) a 1:1 protein to glucose ratio were examined, whereas the physiological concentrations found in the unstressed rat liver (11 μM G-1-P, 0.2 mM G-6-P) were examined for metabolites (15). Ten scans were averaged for the percentage of composition of secondary structures by three different methods (SELCON3, CDSSTR, and CONTIN/LL) with the software package CDPro (16) as previously described (4).

Fluorescent Fatty Acid and Acyl-CoA Binding—PPARα binding affinity for a fluorescent 16 carbon fatty acid analog (BODIPY C-16, Molecular Probes, Eugene, OR) and its CoA thioester (BODIPY C-16-CoA, produced and purified as previously described for acyl-CoAs (4)) was determined. Because of solubility issues with the BODIPY compounds, PPARαΔAB binding affinity was first determined by quenching of intrinsic PPARαΔAB aromatic amino acid fluorescence as described above for glucose. Because both glucose and the BODIPY compounds resulted in quenching of PPARαΔAB intrinsic fluorescence, BODIPY fluorescence was used for determining the effect of glucose on BODIPY fatty acid and fatty acyl-CoA binding. For binding assays, 100 nM PPARαΔAB protein was titrated with increasing concentrations of BODIPY C-16 or BODIPY C-16-CoA in the presence of 6 mM glucose. For displacement assays, binding of 100 nM PPARαΔAB protein with 50 nM BODIPY C-16 or BODIPY C-16-CoA was measured, and the effect of glucose on BODIPY displacement was measured as a decrease in fluorescence intensity. Emission spectra from 490 to 540 nm were obtained at 24 °C by excitation at 460 nm with a PC1 photon counting spectrofluorometer (ISS Inc., Champaign, IL). The data were corrected for background (buffer, fluorescent ligands, and solvent effects), and the maximal intensities were used to calculate the percentage of change in BODIPY C-16 and BODIPY C-16-CoA binding as well as the dissocia-

tion constant (K_d), inhibition constant (K_I), and number of binding sites as previously described (4).

Cell Culture—COS-7 cells (ATCC, Manassas, VA) were grown in DMEM (Invitrogen) supplemented with 10% fetal bovine serum (Invitrogen) at 37 °C with 5% CO_2 in a humidified chamber. Murine L-cell (L arpt$^-$ tk$^-$) fibroblasts were grown as previously described (17).

Coimmunoprecipitation Assays—COS-7 cells were transfected with mammalian expression vectors for full-length PPARα (pSG5-PPARα) (18) and SRC-1 (pcDNA3Δ-SRC-1-Myc) (19) with Lipofectamine 2000 reagent (Invitrogen) according to the manufacturer's instructions. The medium was replaced with serum-free, glucose-free DMEM (Invitrogen) 20 h post-transfection and incubated for an additional 2 h. Cell lysis, coimmunoprecipitation, and Western blot procedures were conducted as previously described for liver homogenate with fatty acyl-CoAs (5). Briefly, 2 mg of cell lysate was mixed with activating ligand and/or glucose as indicated in the figure legend, and the cell lysates were incubated with antibody-linked resin for 1.5 h at room temperature. Eluted proteins were examined by Western blot analysis. The values were normalized to the amount of PPARα protein detected, and the samples in the presence of 10 μM clofibric acid and in the absence of glucose were arbitrarily set to 100%.

NoShift DNA Binding Assays—Full-length PPARα and RXRα RNA was prepared from the mammalian expression plasmids pSG5-PPARα (18) and pSG5-mRXRα (20) and translated with the TNT®-coupled reticulocyte lysate system as recommended by the manufacturer (Promega Corp., Madison, WI). To obtain quantitative data, the NoShift^{TM}II PPAR transcription factor assay kit (Novagen, Madison, WI) was utilized per the manufacturer's instructions with *in vitro* synthesized full-length PPARα (2 μl) and RXRα (2 μl) lysates. Glucose was added to the incubation mixtures as indicated in the figure legend. Luminescence was measured with a Microlite ML3000 microtiter plate luminometer (Dynatech Laboratories, Inc., Chantilly, VA). The values are presented as the percentage of binding where clofibric acid-induced DNA binding (positive control) is arbitrarily set to 100%.

Transactivation Assays—COS-7 cells grown in 6-well culture plates were transfected with 1 μg of each full-length mammalian expression vector (pSG5-PPARα (18) and pSG5-mRXRα (20)) or empty plasmid (pSG5; Stratagene, La Jolla, CA), 1 μg of the reporter construct PPRE$_3$-TK-LUC (21), and 0.05 μg of the internal transfection control plasmid pRL-CMV (Promega Corp., Madison, WI). Transfections were performed with Lipofectamine 2000 reagent (Invitrogen) according to the manufacturer's instructions. Following transfection incubation, the medium was replaced with serum-free, glucose-free DMEM (Invitrogen) for 2 h, and then the ligands were added, and the cells were grown for an additional 24 h. Arachidonic acid was added to cells as a complex with bovine serum albumin as previously described (22). To ensure adequate nuclear levels of these ligands (clofibric acid, arachidonic acid, and glucose) for interaction with PPARα (21, 23, 24), higher concentrations were used for the cell-based transactivation experiments than for the pure protein experiments. Firefly luciferase activity, normalized to *Renilla* luciferase (for transfection efficiency), was

determined with the dual luciferase reporter assay system (Promega, Madison, WI) according to the manufacturer's instructions. Luminescence was measured with a Microlite ML3000 microtiter plate luminometer (Dynatech Laboratories, Inc.).

Determination of Intracellular Glucose Concentration and Nuclear Distribution—COS-7 and L-cells were seeded onto 10-cm culture dishes (for determination of total intracellular glucose concentration) or Lab-Tek chambered cover glass (for determination of nuclear distribution) and cultured as described above for 24 h. The cells were washed two times with PBS and incubated at 37 °C for 3 h in serum-free, glucose-free DMEM (Invitrogen) to ensure utilization of exogenous glucose.

For total intracellular glucose determination and nuclei isolations, the media were replaced with fresh serum-free, glucose-free DMEM supplemented with either 6 μM or 6 mM glucose, and the cells were incubated for an additional 30 min or 2 h at 37 °C. Following incubation, the culture media were removed and examined for glucose content as compared with controls. The cells were washed twice with cold PBS and placed on ice. For total intracellular glucose concentration, the cells were lysed in M-PER® buffer (Pierce) containing 150 mM sodium chloride and protease inhibitors for 10 min at room temperature. Protein content of cell lysate was determined by BCA protein assay (Pierce) and used to estimate total cell number. The nuclei were isolated with the Nuclei EZ Prep nuclei isolation Kit (Sigma) per the manufacturer's instructions. The nuclei were diluted and counted with a hemocytometer according to the manufacturer's instructions (Sigma). Glucose content for cell lysates, nuclei, and cytoplasmic components was determined by the Autokit Glucose CII (Wako Chemicals USA, Richmond, VA) per the manufacturer's instructions.

For determination of glucose distribution, the medium was replaced with PBS containing 1.25 μM Syto59 DNA-binding dye (Molecular Probes, Eugene, OR) and incubated at room temperature for 30 min, and background images were taken. The cells were washed with PBS and incubated at 37 °C for 20 min with PBS containing 6 μM 6-NBD-glucose, a fluorescent, nonhydrolyzable glucose analog (Molecular Probes, Eugene, OR). Following incubation, the cells were washed with PBS and imaged in fresh PBS (see below).

Laser Scanning Confocal Microscopy (LSCM)—LSCM studies were performed with a ×63 Plan-Fluor oil immersion objective, N.A.1.45, an Axiovert 135 microscope (Zeiss, Carl Zeiss Inc., Thornwood, NY), and MRC-1024 fluorescence imaging system (Bio-Rad) as previously described (17). The Syto59 and NBD-glucose probes were excited with laser 488/568 lines with a krypton-argon laser (Coherent, Sunnyvale, CA). Emission from NBD-glucose was recorded by a photomultiplier after passing through a 522/D35 emission filter and emission from Syto59 was collected with a 680/32 emission filter, both under manual gain and black level control. The objective was focused to acquire 0.3-μm confocal slice images through median sections of cells in the field. The cells were excited for 0.1-s intervals, regulated by a computer-controlled shutter and Laser Sharp software (Bio-Rad). The images were analyzed using Image J software from the National Institutes of Health (rsb.info.nih.gov/ij/). The number of pixels of NBD-glucose colocalized with the Syto59 (nuclear localization) as well as the number of NBD-glucose pixels not colocalized with Syto59 (cytoplasmic) were averaged over several replicates ($n = 5$, ~20 cells each) to obtain the percentage of distribution of NBD-glucose.

Calculation of Intracellular and Nuclear Glucose Concentrations—The amount of NBD-glucose in the nucleus was calculated based upon the percentage of distribution (determined by LSCM fluorescence imaging) in nuclei *versus* cytoplasm (plus plasma membrane) from the medial cross-sectional plane. Estimated cellular protein concentration and cellular volumes were as described (25), and final concentrations were calculated from the amount of glucose in the whole cell or nucleus divided by the estimated respective volumes of the whole cell and nucleus. To determine whether NBD-glucose distribution was similar to glucose distribution, the amount of glucose in purified nuclei was compared with the amount of glucose in the cytoplasmic fraction.

Calculation of Nuclear PPARα Concentrations—Liver homogenates from male C57BL/6 mice were prepared and quantified as previously described for coimmunoprecipitation (4). Liver homogenates and known amounts of purified PPARα protein (Novus Biologicals, Littleton, CO) were separated by SDS-PAGE and transferred to nitrocellulose membrane, and Western blot analysis was performed as described previously for PPARα coimmunoprecipitation (4). Protein bands were quantified by densitometry, utilizing a single-chip charge-coupled device video camera FluorChemimager and accompanying FluorChem image analysis software from Alpha Innotech (San Leandro, CA). Total cell number, intracellular volume, and nuclear volume were 1.7×10^8 cells/g of liver, 6.2pL, and 1.8pL, respectively, as determined previously (26, 27). Final concentrations were calculated from the amount of PPARα protein in the whole cell or nucleus divided by the estimated respective volumes of the whole cell and nucleus.

Statistical Analysis—All of the results are expressed as the means ± S.E. Statistical significance between samples in the presence or absence of glucose was determined by using the Student's *t* test with $p < 0.05$.

RESULTS

PPARα Exhibits High Affinity for Glucose and Glucose Metabolites—To determine whether glucose itself directly affects PPARα, PPARα binding of glucose and glucose metabolites was examined. The addition of glucose decreased the intrinsic fluorescence of PPARα, corresponding to ligand binding (4). This change in fluorescence with increasing glucose yielded a sharp saturation curve with a maximal change noted at ~100 nM (Fig. 1*A*), which transformed into a linear reciprocal plot (*inset*), indicating high affinity of PPARα for glucose at a single binding site. Multiple replicates ($n = 4$) yielded a $K_d = 2.0 \pm 0.4$ nM, similar to those obtained previously for unsaturated LCFA and LCFA-CoA (3–5). This is a ligand binding effect, not a covalent modification, because bound radiolabeled glucose was displaced with an excess of nonradiolabeled glucose under the conditions utilized in these assays (data not shown). This suggests that PPARα is highly sensitive to glucose prior to any physical manifestation, such as autoglycation, seen much later in chronic instances such as diabetes. To determine

specificity for glucose, PPARα affinity for glucose-1-phosphate (G-1-P; Fig. 1*B*) and glucose-6-phosphate (G-6-P; Fig. 1*C*) was examined. Both glucose metabolites decreased PPARα fluorescence, indicating strong saturable binding at a single site; G-1-P K_d = 25.3 ± 3.5 nM, G-6-P K_d = 63.2 ± 6.6 nM. These data demonstrate that both glucose and its metabolites directly interact with PPARα with high affinity.

PPARα Binding to Glucose Results in Changes to PPARα Secondary Structure—To determine whether ligand binding altered PPARα conformation, CD was used to determine glucose effects on PPARα secondary structure. The CD spectra of PPARα exhibited a large peak in molar ellipticity at 192 nm and two concomitant negative peaks at 207 and 222 nm (Fig. 1*D* and *E*, *filled circles*). Because maximal glucose binding was noted near a 1:1 glucose to PPARα protein molar ratio, lower (3:4, 0.6 μM, *open circles*) and higher (15:2, 6 μM, *open triangles*) ratios than 1:1 were examined, both resulting in diminished minima and maxima (Fig. 1*D*). Although glucose metabolites (Fig. 1*E*; G-1-P, *open circles*; G-6-P, *open triangles*) significantly altered PPARα spectra in a similar manner as glucose, higher concentrations were required to elicit maximal CD changes, consistent with their weaker affinity. When multiple replicates (n = 3–4) of CD spectra were analyzed for the percentage of composition of α-helices, β-sheets, turns, and unordered structures, the

addition of 0.6 and 6 μM glucose, 11 μM G-1-P, and 0.2 mM G-6-P resulted in similar changes (Table 1). Glucose and the examined metabolites elicited an overall decrease in α-helices, an increase in β-sheets, and increases in turns and unordered structures, similar to the effects of LCFA-CoA binding (4).

Glucose Interferes with PPARα Binding to Fatty Acyl-CoA—Because glucose binding resulted in similar affinities and structural changes as previously reported for LCFA and LCFA-CoA binding, the ability of glucose to alter PPARα interaction with lipidic ligands was examined. PPARα binding of BODIPY-C16, a fluorescent 16 carbon fatty acid analog, was strongly saturable at a single binding site (Fig. 2*C*, *circles*). Binding of the acyl-CoA derivative (BODIPY C-16-CoA) was also strongly saturable at a single binding site (Fig. 2*D*, *circles*). Multiple replicates (n = 4) yielded K_d values or 7.1 ± 1.3 and 17.6 ± 2.4 nM for BODIPY-C16 and BODIPY C-16-CoA, respectively, indicating high binding affinity.

The ability of glucose and glucose metabolites to displace these fluorescent lipids from the PPARα-binding pocket was then examined. Although the addition of glucose, G-1-P, G-6-P, or phosphate (negative control) had only minor effects on BODIPY C-16 fatty acid binding (Fig. 2*A*, *filled bars*), significant differences were noted for BODIPY C-16-CoA (Fig. 2*A*, *open bars*). The addition of 0.6 and 6 mM glucose resulted in significant decreases in acyl-CoA binding, and both G-1-P and G-6-P also significantly decreased acyl-CoA binding but to a lesser extent. Although acyl-CoA displacement leveled off (~35%) by 60 μM glucose, even concentrations as low as 60 nM resulted in significant decreases (Fig. 2*B*). The binding affinity of glucose was found to be slightly lower (K_I = 13.3 ± 1.2 nM) by displacement than that obtained by direct binding. To determine whether glucose changed the binding affinity or simply displaced these lipidic ligands, lipid binding assays were repeated in the presence of excess glucose. Although the shape of the binding curve for BODIPY C-16 in the presence of glucose (Fig. 2*C*, *triangles*) differed slightly from that without glucose, the binding affinity was similar (K_d = 5.0 ± 0.7
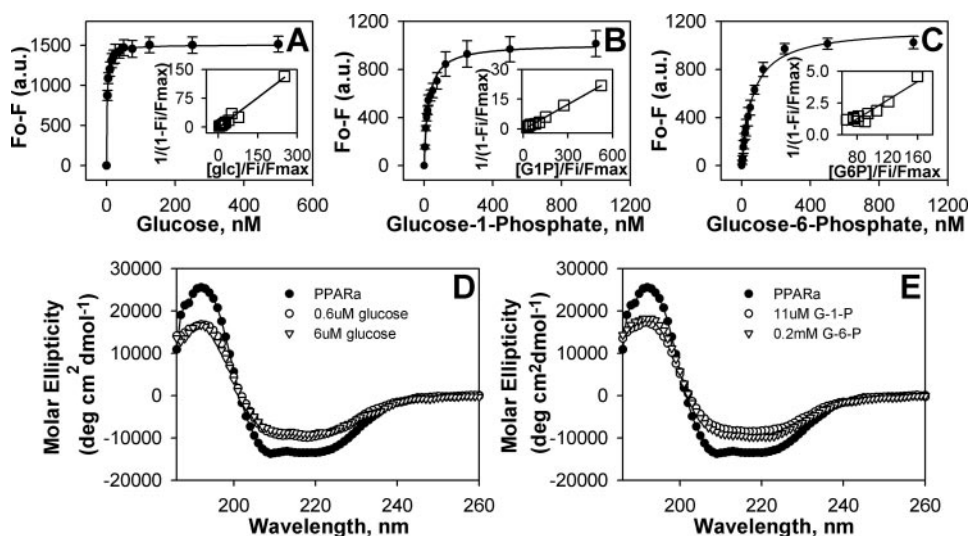

FIGURE 1. **PPARα binds glucose and glucose metabolites with high affinity, resulting in conformational changes.** Binding curve of the change in PPARα intrinsic fluorescence upon titration with glucose (*A*), glucose-1-phosphate (*B*), and glucose-6-phosphate (*C*). The values are presented as the mean value (n = 4) ± the standard error. The *insets* are double reciprocal plots of the mean binding curve data presented in each panel. A representative circular dichroic spectra (n = 3–4, 10 scans each) of PPARα (*D* and *E*, *filled circles*) in the presence of 0.6 μM glucose (*D*, *open circles*); 6 μM glucose (*D*, *open triangles*); 11 μM G-1-P (*E*, *open circles*); and 0.2 mM G-6-P (*E*, *open triangles*).

TABLE 1

Percentage of composition of PPARα secondary structures in the presence of glucose metabolites

The values represent the mean percentages of composition ± the standard error (n = 3–4). Significant differences were determined by Student's *t* test.

|	α-Helices		β-Sheets		Turns	Unordered
	Regular	Distorted	Regular	Distorted		
	%	*%*	*%*	*%*	*%*	*%*
PPARα	23.34 ± 0.28	15.60 ± 0.08	8.29 ± 0.12	6.82 ± 0.08	19.13 ± 0.21	26.86 ± 0.17
0.6 μM glucose	15.23 ± 0.47[a]	12.09 ± 0.22[a]	13.14 ± 0.87[a]	8.43 ± 0.29[a]	21.61 ± 0.53[a]	29.11 ± 0.56[a]
6 μM glucose	15.71 ± 0.22[a]	12.57 ± 0.13[a]	12.77 ± 0.65[a]	8.58 ± 0.22[a]	21.53 ± 0.41[a]	28.00 ± 0.50[a]
11 μM G-1-P	13.47 ± 0.35[a]	11.40 ± 0.31[a]	14.53 ± 0.91[a]	8.71 ± 0.30[a]	21.66 ± 0.44[a]	29.96 ± 0.58[a]
0.2 mM G-6-P	17.21 ± 0.38[a]	12.83 ± 0.16[a]	12.08 ± 0.81[a]	8.14 ± 0.23[a]	21.34 ± 0.61[a]	28.87 ± 0.87[a]

[a] $p < 0.01$.
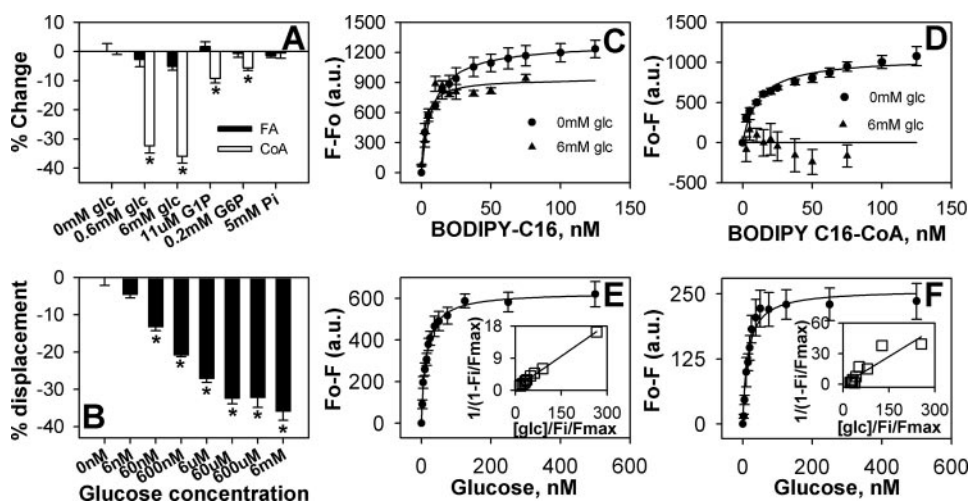
FIGURE 2. **Glucose binding inhibits fatty acid metabolite binding but lipid binding does not inhibit glucose binding.** The percentage of change in PPARα binding to BODIPY C-16 fatty acid (*filled bars*) and BODIPY C-16-CoA (*open bars*) in the presence of glucose and glucose metabolites (*A*). Examination of the effect of lower concentrations of glucose on PPARα binding to BODIPY C-16-CoA (*B*) shows that this effect is saturable, allowing for calculation of glucose affinity by BODIPY C-16-CoA displacement as described under "Experimental Procedures." Binding of PPARα to BODIPY C-16 fatty acid (*C*) is similar in the absence (*circles*) and presence of 6 mM glucose (*triangles*), both resulting in high affinity binding. Binding of PPARα to BODIPY C-16-CoA (*D*) in the absence (*circles*) of glucose results in strong binding, whereas the presence of 6 mM glucose (*triangles*) results in no BODIPY C-16 CoA binding. Glucose binding in the presence of 10 μM BODIPY C-16 fatty acid (*E*) and BODIPY C-16-CoA (*F*) still shows strong saturable binding. The values are the mean values (*n* = 4–5) ± the standard error. *Insets*, double reciprocal plots of the mean binding curve data. *Asterisks* represent significant deviation from no glucose controls ($p < 0.05$).

nM). In contrast, no BODIPY C-16-CoA binding was noted in the presence of glucose (Fig. 2*D*, *triangles*). Although the presence of excess BODIPY C-16 fatty acid (Fig. 2*E*) or acyl-CoA (Fig. 2*F*) did not prevent glucose binding, a 6–7-fold decrease in glucose affinity was noted (K_d values of 13.8 ± 1.8 and 14.6 ± 3.4 nM, respectively). This is similar to the affinity obtained for glucose through the displacement of BODIPY C-16-CoA.

Glucose Decreases Coactivator Recruitment of PPARα under Basal Conditions while Increasing Coactivator Recruitment of PPARα in the Presence of Activating Lipidic Ligands—In homogenates from COS-7 cells grown in serum-free, glucose-free medium, the addition of glucose decreased PPARα interaction with the steroid receptor coactivator-1 (SRC-1) in a concentration-dependent manner (Fig. 3*A*). Although larger concentrations of glucose inhibited PPARα interaction with SRC-1 more than weaker concentrations, even 0.6 μM glucose resulted in a significant decrease in SRC-1 recruitment, suggesting that glucose inhibits PPARα regulated transcription in the absence of other ligands. In contrast, in homogenates from COS-7 cells incubated with arachidonic acid (Fig. 3*B*) or clofibric acid (Fig. 3*C*), low levels of glucose (6 μM) significantly increased PPARα interaction with SRC-1, whereas higher concentrations of glucose (above 60 μM) did not alter SRC-1 recruitment. This suggests that PPARα may regulate both lipid and sugar metabolism through a ligand concentration-dependent selection.

Glucose Increases PPARα-RXRα Binding to DNA—Because PPARα heterodimerization to RXRα increases DNA binding (21), *in vitro* synthesized PPARα and RXRα protein was used to determine the effect of glucose on DNA binding. To quantitate this effect of DNA binding, a NoShift assay was utilized. Under basal conditions, the addition of glucose (6 nM to 6 mM) resulted in more DNA binding by PPARα-RXRα than seen in the absence of glucose (Fig. 3*D*). This effect of DNA binding increased with increasing glucose concentrations, with the effect plateauing around 6 μM. In the presence of arachidonic acid, the addition of glucose increased DNA binding until 0.6 μM, at which point DNA binding plateaued (Fig. 3*E*). In the presence of clofibric acid, the addition of glucose increased DNA binding until about 60 nM (Fig. 3*F*). In each case, the addition of glucose significantly increased PPARα-RXRα heterodimer binding to the PPRE.

Glucose Increases Transactivation of PPARα-RXRα Heterodimers—Because PPARα forms heterodimers with RXRα to induce transactivation (21, 23), the cells were cotransfected with PPARα alone, RXRα alone, PPARα and RXRα, or pSG5 empty vector. PPARα transactivation was measured as response of firefly luciferase upon interaction of PPARα with the PPRE of the acyl-CoA oxidase promoter (21) normalized to *Renilla* luciferase. Although only slight changes in transactivation of the acyl-CoA oxidase luciferase fusion protein were noted for the addition of glucose to PPARα in the absence of RXRα or added lipidic ligands, concentrations between 0.6 and 2.4 mM resulted in decreased activation, whereas 6 mM glucose had no effect (Fig. 3*G*). Similar results were obtained in the presence of 10 μM arachidonic acid (Fig. 3*H*). However, the addition of 10 μM clofibric acid resulted in approximately a 3-fold increase in activation but only at 6 mM glucose (Fig. 3*I*). Glucose had no significant effect on RXRα transactivation (Fig. 3, *G–I*).

In the presence or absence of clofibric acid, transcriptional activity of PPARα was increased ~3.7-fold by the presence of RXRα (Fig. 3, *G* and *I*, *open bars*), whereas in the presence of arachidonic acid, transcription only increased 2.5-fold (Fig. 3*H*, *open bars*). The addition of glucose increased transcriptional activity of PPARα-RXRα heterodimers in both the presence and absence of ligands. In the absence of ligand, PPARα-RXRα activity increased with increasing glucose concentration from 0.6 to 2.4 mM, whereas activity levels were only slightly higher with 6 mM glucose than in the absence of glucose (Fig. 3*G*). Arachidonic acid-induced activity was increased 1.4-fold with the addition of 2.4 mM glucose and almost 3-fold with 6 mM glucose (Fig. 3*H*). Clofibric acid-induced activity increased with increasing glucose concentration, with 6 mM glucose resulting in a 2.5-fold increase (Fig. 3*I*). Although arachidonic acid-induced expression resulted in the largest change compared with no glucose controls, clofibric-acid induced expression in the presence of 6 mM glucose resulted in the highest amount of expression.
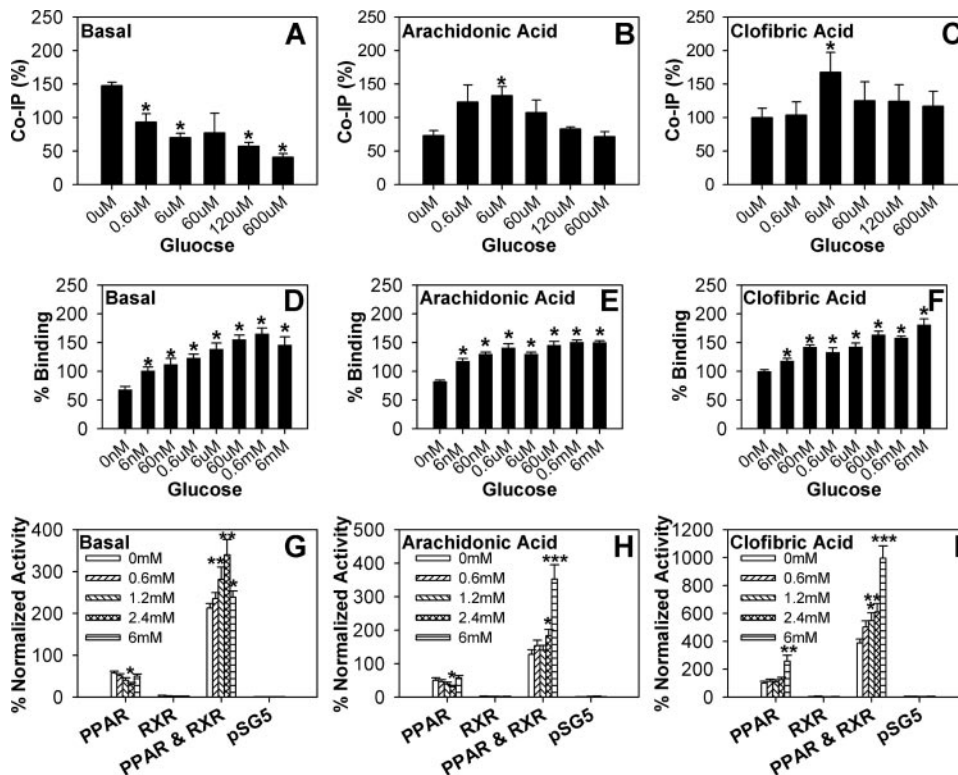
FIGURE 3. **Glucose alters PPARα interaction with coactivators, DNA binding, and transactivation.** COS-7 cells were transfected with mammalian expression vectors for PPARα and SRC-1 as described under "Experimental Procedures." Glucose was added to cell lysates, and the effect of glucose on coimmunoprecipitation of SRC-1 with PPARα in the absence (*A*) or presence of activating ligands (arachidonic acid, *B*; clofibric acid, *C*). The values were normalized to the amount of PPARα protein detected, and the samples in the presence of 10 μM clofibric acid and in the absence of glucose were arbitrarily set to 100%. The effect of glucose on PPARα-RXRα heterodimer DNA binding with a quantitative NoShiftII assay (Novagen) under basal (*D*), arachidonic acid-induced (*E*), and clofibric acid-induced (*F*) conditions. The values are presented as percentages of binding where clofibric acid-induced DNA binding (positive control) is arbitrarily set to 100%. COS-7 cells transfected with PPARα, RXRα, PPARα, and RXRα, or control pSG5 empty vector were analyzed for basal (*G*), 10 μM arachidonic acid-induced (*H*), and 10 μM clofibric acid-induced (*I*) transactivation of an acyl-CoA oxidase reporter construct in the presence of 0 mM glucose (*open bars*), 0.6 mM glucose (*diagonally upward bars*), 1.2 mM glucose (*diagonally downward bars*), 2.4 mM glucose (*hatched bars*), and 6 mM glucose (*horizontally lined bars*). The transactivation values are presented as percentages of firefly luciferase activity normalized to *Renilla* luciferase (internal control) where clofibric acid-induced PPARα activity in the absence of glucose (positive control) is arbitrarily set to 100%. The bar graph values represent the mean values (*n* = 3) ± the standard error. *Asterisks* represent significant differences for the addition of glucose ($p < 0.05$).

ranged from 25 to 47 μM, whereas nuclear concentrations ranged from 6 to 22 μM, depending upon the cell line and the length of incubation (Table 3). By Western blot analysis (Fig. 4*E*), PPARα constitutes ~1.6 ± 0.2% of total liver proteins. Because the majority of PPARα protein is nuclear in cultured L-cell fibroblasts (25) and cultured mouse primary hepatocytes (28),[3] the estimated nuclear concentration of PPARα was 309 ± 28 μM.

DISCUSSION

Although several studies have suggested that PPARα may function to regulate glucose homeostasis, it was believed that such regulation occurred only as an indirect action of fatty acid on PPARα. Because hallmarks of ligand-activated nuclear receptors are high ligand affinity, ligand-induced conformational change, and ligand-induced alteration in receptor activity, the experiments herein demonstrate for the first time that glucose itself is an endogenous ligand of PPARα. Furthermore, glucose was able to alter the effects of other endogenous PPARα ligands by inhibiting LCFA-CoA binding while enhancing the transcriptional effects of fatty acids.

Because the first step of β-oxidation is the conversion of LCFA to LCFA-CoA, it may seem counterintuitive that the presence of glucose decreased the affinity of PPARα for

Nuclear Glucose Concentration Is in the Low Micromolar Range while PPARα Concentration Is ~10-fold Higher—Because of the inability to remove all serum from liver tissues by a noninvasive technique (*i.e.* without disrupting the cellular glucose equilibrium) and because serum glucose levels are in the millimolar range (15), cultured cells were used as a model to estimate total intracellular and nuclear glucose levels in the presence of 6 μM and 6 mM extracellular glucose. Intracellular glucose was determined by a chemical assay, whereas nuclear distribution was determined by a noninvasive LSCM technique, as described under "Experimental Procedures." LSCM of NBD-glucose showed that ~11.3% of the intracellular NBD-glucose was nuclear in COS-7 cells (Fig. 4, *A* and *C*), whereas only 5.9% NBD-glucose was nuclear in L-cells (Fig. 4, *B* and *D*). A similar distribution was obtained when nuclei and cytoplasmic fractions were examined by chemical assay under the same conditions (*i.e.* 6 μM glucose and 30 min incubation), although some variation was noted between 30-min and 2-h incubations (Table 2). The estimated intracellular glucose concentrations

fatty acyl-CoA ligands while increasing PPARα activation of a β-oxidation enzyme. However, it should be noted that not only LCFA-CoAs but also unsaturated LCFA are PPARα activators (3–5, 29–31), and LCFA binding to PPARα was unaltered by the presence of glucose. Further, in the absence of RXRα, the addition of glucose to PPARα (with or without added arachidonic acid) resulted in decreased activation of the β-oxidation enzyme. Only in the presence of clofibric acid, a very potent PPARα agonist, was an increase in activation seen. Earlier experiments (32, 33) have suggested that although LCFA binding induces PPARα activation (agonists), a nonhydrolyzable LCFA-CoA represses PPARα activity (antagonists). Thus, it is possible that glucose binding may function as a rheostat-like control mechanism to regulate LCFA or LCFA-CoA binding to PPARα.

Sequence comparisons of the binding sites of several glucose-binding proteins suggest that three amino acids (aspara-

---

[3] A. L. McIntosh, B. P. Atshaves, H. Huang, H. R. Payne, H. A. Hostetler, J. Davis, A. B. Kier, and F. Schroeder, unpublished observation.
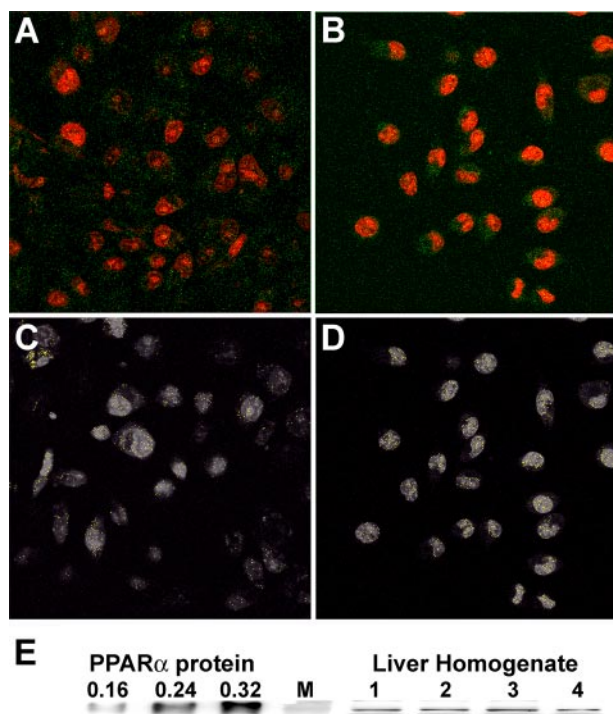
FIGURE 4. **Nuclear glucose concentration was determined by NBD-glucose localization in cultured fibroblasts.** A representative image ($n = 5$) for each cell line is presented. COS-7 (*A* and *C*) and L-cells (*B* and *D*) were incubated for 30min with NBD-glucose (*green pixels*), stained with the nuclear dye SYTO59 (*red pixels*), and imaged by LSCM as described under "Experimental Procedures." Colocalized pixels (*C* and *D*, *yellow pixels*) were measured and represent nuclear NBD-glucose. NBD-glucose not colocalizing with SYTO59 was measured as cytoplasmic. *E*, Western blot of 10 μg samples of total protein from mouse liver homogenates ($n = 4$) as compared with known concentrations (0.16, 0.24, and 0.32 μg) of purified recombinant PPARα protein as a control to determine the relative amount of PPARα in liver cells. Protein molecular mass marker (*lane M*) band approximately equals 50 kDa.

TABLE 2

Percentage of distribution of glucose in cultured cells by chemical analysis of purified nuclei and cytoplasmic fractions

The values represent the mean percentages of glucose ($n = 4 – 6$) in each fraction ± the standard error.

	Glucose concentration for incubation	30 min of incubation		2 h of incubation	
		Cytoplasmic	Nuclear	Cytoplasmic	Nuclear
		%		*%*	
COS-7 cells	6 μM	88.7 ± 1.3	11.3 ± 1.3	95.5 ± 0.2	4.5 ± 0.2
	6 mM	93.5 ± 1.2	6.5 ± 1.2	95.9 ± 0.9	4.1 ± 0.9
L-cells	6 μM	94.5 ± 0.6	5.5 ± 0.6	95.3 ± 0.8	4.7 ± 0.8
	6 mM	93.2 ± 4.5	6.8 ± 4.5	92.6 ± 2.1	7.4 ± 2.1

TABLE 3

Estimated intracellular and nuclear glucose concentrations in cultured cells

The values represent the mean glucose concentrations ($n = 4$) ± the standard error.

	Glucose concentration for incubation	Intracellular glucose concentration		Nuclear glucose concentration	
		30 min of incubation	2 h of incubation	30 min of incubation	2 h of incubation
		μM		*μM*	
COS-7 cells	6 μM	36.56 ± 1.89	31.91 ± 1.08	17.95 ± 0.93	15.66 ± 0.53
11.3%	6 mM	41.40 ± 4.19	45.49 ± 1.88	20.32 ± 2.06	22.33 ± 0.92
L-cells	6 μM	47.43 ± 5.88	24.71 ± 2.85	12.08 ± 1.50	6.30 ± 0.73
5.9%	6 mM	35.36 ± 1.22	29.87 ± 7.34	9.01 ± 0.18	7.61 ± 1.87

gine, aspartic acid, and glutamic acid) are essential for glucose binding (34). The PPARα crystal structure (35) contains numerous asparagine, aspartic acid, and glutamic acid residues within the ligand-binding domain. If glucose and the CoA moiety of fatty acyl-CoA both bind to these residues, then glucose could prevent the fatty acyl-CoA from fitting into the PPARα-binding pocket, while not disturbing fatty acid binding. Because the presence of glucose reduces acyl-CoA binding affinity, only the fatty acid would still be capable of binding to PPARα to affect downstream regulation at elevated glucose concentrations. This has two important potential consequences: (i) because saturated fatty acids do not directly bind or activate PPARα (3–5), the response to dietary fat (saturated *versus* unsaturated) may be altered and (ii) high levels of glucose and fatty acid may result in hyperactivation of PPARα (36).

Although the exact concentrations of glucose, glucose metabolites, and PPARα protein in cells expressing PPARα is unknown and likely varies with diet, we have attempted to estimate these values to better relate the recombinant PPARα protein ligand affinity to the more physiological experiments. The total amount of nuclear glucose was estimated to be in the micromolar range, similar to the glucose concentration noted for maximal changes in coactivator recruitment of PPARα in the presence of arachidonic acid and clofibric acid, and well within the range of glucose concentrations responsible for altering DNA binding. However, the proportion of the nuclear glucose available for interaction with PPARα remains unknown. Because other proteins besides PPARα can bind to glucose, it is possible that free nuclear glucose levels are substantially lower. For example, the liver fatty acid binding protein (L-FABP) is known to interact with glucose (15), and liver cell concentrations of L-FABP are high, in the range of 200–400 μM, whereas nuclear concentrations of L-FABP are estimated to be ~43 μM (17, 25). This suggests the existence of dynamic interrelationships between glucose, lipidic ligands (LCFA, LCFA-CoA, fibrates, etc.), and binding proteins in the nucleus (PPARα, L-FABP, etc.).

Although the glucose concentrations utilized for the cell-based and cell lysate-based assays are higher than those used for the pure PPARα based assays, it should be noted that this is the applied glucose concentration and does not necessarily represent the concentration of glucose available to interact with PPARα. Intracellular glucose concentration is a function not only of glucose supply (*i.e.* extracellular glucose concentration) but also of the rate of glucose transport across the plasma membrane and the rate of glucose metabolism (37, 38). Because the rate of glucose transport into the cell is limited by the isoform type, number, and affinity of glucose transporters present at the cell surface (38), the intracellular glucose concentration is expected to vary between cell types and might be lower for cultured cells than for liver tissue. Moreover, the presence of hexokinases within the cells would rapidly convert free glucose into glucose-6-phosphate, again altering the intracellular or nuclear glucose levels available for interaction with PPARα. Consequently, not only for cell-based assays but also for cell lysate-based assays, additional factors may contribute to the higher glucose concentration needed to elicit significant effects as compared with *in vitro* pure PPARα based assays. This would

include: (i) endogenous glucose; (ii) glucose metabolites such as G-6-P and G-1-P, both of which are bound by PPARα, albeit more weakly; (iii) additional proteins that also bind glucose (*e.g.* plasma membrane glucose transporters, hexokinase, nuclear proteins, etc.); (iv) competition of SRC-1 binding with other coactivators and corepressors; and (v) competition with other nuclear proteins that may compete with PPARα for binding to DNA (*e.g.* HNF4α in liver). Consequently, the cell lysate-based assays require considerably higher levels of glucose, and the changes elicited tend to be smaller. These issues are analogous to those observed for PPARα-binding fatty acids and fatty acyl-CoAs with nM K_d values, whereas cell lysate-based assays (cofactor recruitment) required 100–1000-fold higher concentrations (3–5, 33).

Because glucose effects on transactivation of PPARα and RXRα heterodimers were concentration-dependent, this suggests that PPARα is not saturated at the lower end of physiological or dietary levels of glucose, even though the affinity of PPARα for glucose is very high. Furthermore, this suggests that the free nuclear levels of glucose are low and less than the nuclear PPARα levels. A parallel situation exists for PPARα and fatty acid activation. Although PPARα affinities for fatty acids and their metabolites (*i.e.* fatty acyl-CoAs) are in the low nanomolar range (3–5), transactivation assays and animal studies show that PPARα is activated by physiological (μM) and dietary (mM) levels of fatty acids (29–31, 39). Serum levels for fatty acids range from 0.3 to 1 mM depending on nutrient and/or diabetic status. However, free nuclear LCFA and LCFA-CoA concentrations are estimated to be in the range of 39–68 nM and 3 nM, respectively (17, 25). Such discrepancies between binding affinity and ligand concentration required for PPARα transactivation and activation are most likely due to higher concentrations of PPARα than free ligand within the nucleus.

Further, several studies suggest that glucose binding to PPARα shown herein occurs at physiologically relevant glucose concentrations. Unlike most cells, liver cells express very high levels of PPARα (300 μM as estimated herein) and are freely permeable to glucose (40). Tissues other than liver are more insulin-responsive and have much lower intracellular glucose levels. For example, nuclear magnetic resonance imaging of muscle from normal and diabetic subjects showed that intracellular glucose concentrations were several orders of magnitude lower than in plasma (41). In muscle tissues, glucose and glucose metabolite levels are much closer to the respective affinities of PPARα for these ligands. The effects of glucose on PPARα binding to LCFA and LCFA-CoA were well within the range of nuclear LCFA and LCFA-CoA levels (17, 25). Liver homogenates contain 6 mM glucose, 11 μM G-1-P, and 0.2 mM G-6-P total concentrations (15). These data suggest that depending on tissue type, the effects of both low and high glucose level may be physiologically significant.

Further, either nonspecific effects of high glucose or additional effects of glucose metabolites may also contribute lysate-based assays. With regards to the latter, for example, G-1-P shows effects at 11 μM glucose. Thus, this glucose metabolite may be as physiologically relevant as glucose (or G-6-P) in interacting with PPARα. It is possible that at low glucose levels, glucose itself is interacting with PPARα, whereas at higher glucose concentrations, the G-1-P or other metabolite may be interacting with PPARα.

However, it is possible that in some cell types or tissues, free nuclear glucose concentrations are at a PPARα saturating level. If in the future it is found that this is true, then this would indicate that the glucose-saturated PPARα would be the physiological form for those cell types or tissues. Therefore, PPARα assays would need to include saturating levels of glucose to be physiologically relevant with these cell types. Because glucose can enter liver cells though diffusion (40), liver may have elevated intracellular glucose levels, whereas other tissues may be glucose-deficient. In this case, perhaps altered nuclear glucose levels lead to the improper PPARα activation found in diabetic patients (36, 42).

The data presented herein suggest a mechanistic role of PPARα in the regulation of energy homeostasis by directly linking glucose and fatty acid oxidation. Previous work has shown that PPARα is capable of binding fatty acyl-CoAs and unsaturated fatty acids with very high affinity (3–5). The data provide evidence that PPARα also directly interacts with glucose and glucose metabolites with very high affinity, well within the range of normal physiological levels of these molecules in serum, cytoplasm, and nucleoplasm (15, 40, 41). This interaction altered PPARα secondary structure and the ability of PPARα to interact with lipidic ligands. Under basal conditions, glucose decreased PPARα interaction with SRC-1 while increasing interaction with DNA. In the presence of activating ligands (fatty acids, fibrates), glucose increased PPARα interaction with SRC-1, DNA binding, and activation of the $β$-oxidation pathway. These results suggest that hyperglycemic injury mediated by PPARα occurs not only indirectly through elevated LCFA and LCFA-CoA levels but also as a direct action of glucose on PPARα and through synergistic effects with xenobiotic and endogenous PPARα activators.

REFERENCES

1. Zhang, Y., Lee, F. Y., Barrera, G., Lee, H., Vales, C., Gonzalez, F. J., Willson, T. M., and Edwards, P. A. (2006) *Proc. Natl. Acad. Sci. U. S. A.* **103,** 1006–1011
2. Kersten, S., Mandard, S., Escher, P., Gonzalez, F. J., Tafuri, S., Desvergne, B., and Wahli, W. (2001) *FASEB J.* **15,** 1971–1978
3. Lin, Q., Ruuska, S. E., Shaw, N. S., Dong, D., and Noy, N. (1999) *Biochemistry* **38,** 185–190
4. Hostetler, H. A., Petrescu, A. D., Kier, A. B., and Schroeder, F. (2005) *J. Biol. Chem.* **280,** 18667–18682
5. Hostetler, H. A., Kier, A. B., and Schroeder, F. (2006) *Biochemistry* **45,** 7669–7681
6. Corkey, B. E., Deeney, J. T., Yaney, G. C., and Tornheim, K. (2000) *J. Nutr.* **130,** 299S–304S
7. Mangelsdorf, D. J., and Evans, R. M. (1995) *Cell* **83,** 841–850
8. Desvergne, B., Michalik, L., and Wahli, W. (2004) *Mol. Endocrinology* **18,** 1321–1332

9. Frederiksen, K. S., Wulf, E. M., Wassermann, K., Sauerberg, P., and Fleckner, J. (2003) *J. Mol. Endocrinol.* **30,** 317–329
10. Kiec-Wilk, B., Dembinska-Kiec, A., Olszanecka, A., Bodzioch, M., and Kawecka-Jaszcz, K. (2005) *J. Phys. Pharm.* **56,** 149–162
11. Guerre-Millo, M., Rouault, C., Poulain, P., Andre, J., Poitout, V., Peters, J. M., Gonzalez, F. J., Fruchart, J.-C., Reach, G., and Staels, B. (2001) *Diabetes* **50,** 2809–2814
12. Forman, B. M., Tontonoz, P., Chen, J., Brun, R. P., Spiegelman, B. M., and Evans, R. M. (1995) *Cell* **83,** 803–812
13. Kliewer, S. A., Lenhard, J. M., Willson, T. M., Patel, I., Morris, D. C., and Lehmann, J. M. (1995) *Cell* **83,** 813–819
14. Hi, R., Osada, S., Yumoto, N., and Osumi, T. (1999) *J. Biol. Chem.* **274,** 35152–35158
15. Stewart, J. M., Dewling, V. F., and Wright, T. G. (1998) *Biochim. Biophys. Acta* **1391,** 1–6
16. Sreerama, N., and Woody, R. (2000) *Anal. Biochem.* **287,** 252–260
17. Huang, H., Starodub, O., McIntosh, A., Kier, A. B., and Schroeder, F. (2002) *J. Biol. Chem.* **277,** 29139–29151
18. Patsouris, D., Mandard, S., Voshol, P. J., Escher, P., Tan, N. S., Havekes, L. M., Koenig, W., Maerz, W., Tafuri, S., Wahli, W., Mueller, M., and Kersten, S. (2004) *J. Clin. Investig.* **114,** 94–103
19. Yao, T.-P., Ku, G., Zhou, N., Scully, R., and Livingston, D. M. (1996) *Proc. Natl. Acad. Sci. U. S. A.* **93,** 10626–10631
20. Leid, M., Kastner, P., Lyons, R., Nakshatri, H., Saunders, M., Zacharewski, T., Chen, J. Y., Staub, A., Garnier, J. M., Mader, S., and Chambon, P. (1992) *Cell* **58,** 377–395
21. Kliewer, S. A., Umesono, K., Noon, D. J., Heyman, R. A., and Evans, R. M. (1992) *Nature* **358,** 771–774
22. Spector, A. A., and Hoak, J. C. (1969) *Anal. Biochem.* **32,** 297–302
23. Keller, H., Dreyer, C., Medin, J., Mahfoudi, A., Ozato, K., and Wahli, W. (1993) *Proc. Natl. Acad. Sci. U. S. A.* **90,** 2160–2164
24. Gottlicher, M., Widmark, E., Li, Q., and Gustafsson, J. A. (1992) *Proc. Natl. Acad. Sci. U. S. A.* **89,** 4653–4657
25. Huang, H., Starodub, O., McIntosh, A., Atshaves, B. P., Woldegiorgis, G., Kier, A. B., and Schroeder, F. (2004) *Biochemistry* **43,** 2484–2500
26. Drochmans, P., Wanson, J.-C., and Mosselmans, R. (1975) *J. Cell Biol.* **66,** 1–22
27. Buira, I., Poch, E., Sanchez, O., Fernandez-Varo, G., Grau, M., Tebar, F., Ramirez, I., and Soley, M. (2004) *J. Cell Physiol.* **198,** 12–21
28. Wolfrum, C., Borrmann, C. M., Borchers, T., and Spener, F. (2001) *Proc. Natl. Acad. Sci. U. S. A.* **98,** 2323–2328
29. Wolfrum, C., Ellinghaus, P., Fobker, M., Seedorf, U., Assmann, G., Borchers, T., and Spener, F. (1999) *J. Lipid Res.* **40,** 708–714
30. Krey, G., Braissant, O., L'Horset, F., Kalkhoven, E., Perroud, M., Parker, M. G., and Wahli, W. (1997) *Mol. Endocrinol.* **11,** 779–791
31. Banner, C. D., Gottlicher, M., Widmark, E., Sjovall, J., Rafter, J. J., and Gustafsson, J. (1993) *J. Lipid Res.* **34,** 1583–1591
32. Murakami, K., Ide, T., Nakazawa, T., Okazaki, T., Mochizuki, T., and Kadowaki, T. (2001) *Biochem. J.* **353,** 231–238
33. Elholm, M., Dam, I., Jorgenesen, C., Krogsdam, A.-M., Holst, D., Kratchamarova, I., Gottlicher, M., Gustafsson, J. A., Berge, R. K., Flatmark, T., Knudsen, J., Mandrup, S., and Kristiansen, K. (2001) *J. Biol. Chem.* **276,** 21410–21416
34. Li, T., Lee, H. B., and Park, K. (1998) *J. Biomater. Sci. Polym. Ed.* **9,** 327–344
35. Cronet, P., Peterson, J. F. W., Folmer, R., Blomberg, N., Sjoblom, K., Karlsson, U., Lindstedt, E.-L., and Bamberg, K. (2001) *Structure* **9,** 699–706
36. Finck, B. N., Lehman, J. J., Leone, T. C., Welch, M. J., Bennett, M. J., Kovacs, A., Han, X., Gross, R. W., Kozak, R., Lopaschuk, G. D., and Kelly, D. P. (2002) *J. Clin. Investig.* **109,** 121–130
37. Fehr, M., Lalonde, S., Lager, I., Wolff, M. W., and Frommer, W. B. (2003) *J. Biol. Chem.* **278,** 1927–19133
38. Wasserman, D. H., and Halseth, A. E. (1998) *Adv. Exper. Med. Biol.* **441,** 1–16
39. Bonilla, S., Redonnet, A., Noel-Suberville, C., Pallet, V., Garcin, H., and Higueret, P. (2000) *Br. J. Nutr.* **83,** 665–671
40. Voet, D., and Voet, J. G. (1990) *Biochemistry* (Voet, D., and Voet, J. G., eds) John Wiley & Sons, New York
41. Cline, G. W., Petersen, K. F., Krssak, M., Shen, J., Hundal, R. S., Trajanoski, Z., Inzucchi, S., Dresner, A., Rothman, D. L., and Shulman, G. I. (1999) *N. Engl. J. Med.* **341,** 240–246
42. Finck, B. N. (2004) *Curr. Op. Clin. Nutr. Metab. Care* **7,** 391–396